

## CHAPTER 4

### Experimental Results

#### 4.1 Crack development

Figures 4.1 illustrate the crack pattern of all specimens developed from low loading to the high drift level. For all specimens, flexural cracks on the beams were firstly observed at the potential plastic hinge regions located at distances of  $d/2 - d$  (effective beam depth) from the beam-column interfaces. With an increasing of the drift level, those cracks further propagated and a few flexural cracks also developed on the concrete columns above and below the joint region. Then, the first diagonal cracks on the beam-column joint core appeared. The cracking development from the drift larger than 1.00% of all the specimens were different due to the different reinforcement details in the joint region. For the monolithic specimen M1 as shown in Figure 4.1(a), major cracking was the flexural cracks in the beams near the column faces and there were a few diagonal cracks within the concrete joint. Only a limited number of flexural cracks appeared in the columns immediately above and below joint. When the drift level reached 3.50%, crushing of the concrete cover at the bottom of beams began and the beam bottom longitudinal bars buckled at a 4.00% drift level.

For the Gravity precast concrete connection specimen (P1), laterally splitting cracks running parallel to the T-section steel, installed at the middle beam depth, close to column face started at the 1.00% drift level. When the drift level was increased to 1.40%, the first splitting cracks formed at distances of  $d$  from the column faces along the lap-splices of the main longitudinal bars at the top section of both beams. By increasing the drift level up to 2.00-3.50%, the splitting cracks were gradually propagated and opened wider than 2.0 mm. In addition, the new flexural cracks on both beams were distinctly observed at the potential plastic hinge regions near column face and no cracks appeared in the column. The splitting cracks at the top and middle of the beam cross section near

the column face resulted in a dramatic decrease in the shear capacity. Figure 4.1(b) shows the crack patterns of specimen P1 during the cyclic loading test.

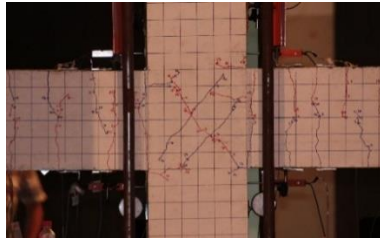
In specimen P2, at a drift level of 1.00% visible lateral cracks were observed at the bottom of both beams and the joint core at the beam-column interface. A few splitting cracks appeared parallel to lap-splices and main longitudinal bars at the top beam section, which were initiated at distances of 250 mm ( $d$ ) away from the column faces. When increasing to a drift level of 1.40%, cracks were gradually propagated along the lateral directions, as the drift levels were increased. When the drift level reached to 3.50%, the concrete of the top beam section close to the beam-column joint started to crush and spall along the splitting crack. Similar to specimen P1, no cracks appeared on either the top or bottom columns, as shown in Figure 4.1(c).

Specimens P3 and P4 also showed similar crack patterns as P2 as shown in Figure 4.1(d-e). The main failure modes were initiated from the bond splitting cracks occurred along the lap-splices at the top beam section in the cast-in-place grout concrete regions.

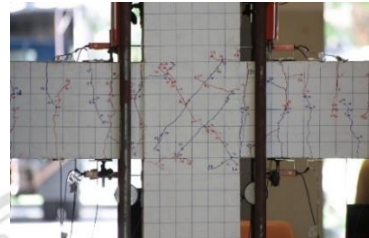
For specimen P5, the splitting cracks appeared parallel to the steel T-section and the main longitudinal bars were initiated at the bottom beam section close to the column faces, as the drift level increased to 1.40%. With the increase in the drift level the splitting cracks further propagated. The concrete below the T - section steel at the bottom beam section close to the beam-column joint were crushed and spalled. At a distance of about the beam depth from the column face of both precast beams the flexural cracks were very large. Figure 4.1(f) shows the crack distribution of the specimens after testing.

Regard to the cracking development of the P6 precast specimen, the horizontal cracks in level of cover concrete on top beam region located around the distant  $d$  away from the precast column were observed. A few spalling concrete cover in bottom precast beam region were investigated at the story drift level of 2.50%, coinciding the edge of T-section steel insert in precast beams. When the drift level reached 3.50%, the flexural cracks of beam elements located around 20-25 cm away from the column face were opened approximately 2.0 mm width, widening of the cracks accelerated at repeated cycle in the same drift level. Also, the horizontal cracks which was wider than 2.0 mm further propagated, running from the column face along 25 cm to the flexural beam cracks. At

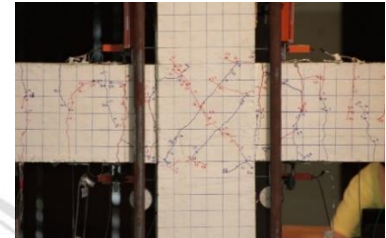
the first cycle of the 4.50% story drift level, concrete beam structures at the edges of T-section were separated due to the flexural crack opening. Afterward, the spalling of concrete cover on the top and bottom beam regions and other spalling of concrete cover spread on the beam surfaces at the location were pronounce as shown in Figure 4.1(g).



Drift ratio = 1.00%



Drift ratio = 2.00%



Drift ratio = 2.50%

(a) Specimen M1



Drift ratio = 1.00%



Drift ratio = 2.00%

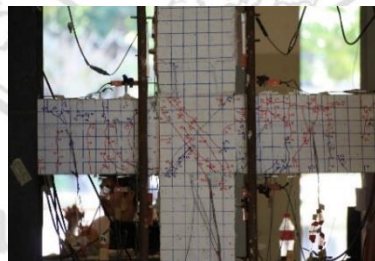


Drift ratio = 2.50%

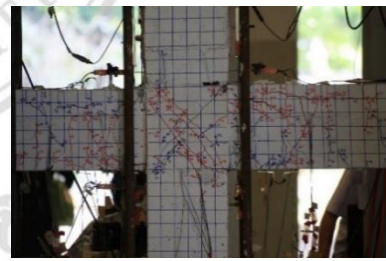
(b) Specimen P1



Drift ratio = 1.00%

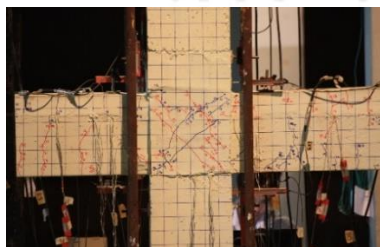


Drift ratio = 2.00%

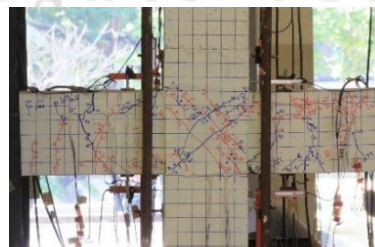


Drift ratio = 2.50%

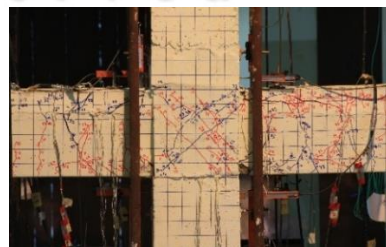
(c) Specimen P2



Drift ratio = 1.00%



Drift ratio = 2.00%



Drift ratio = 2.50% (Failure)

(d) Specimen P3

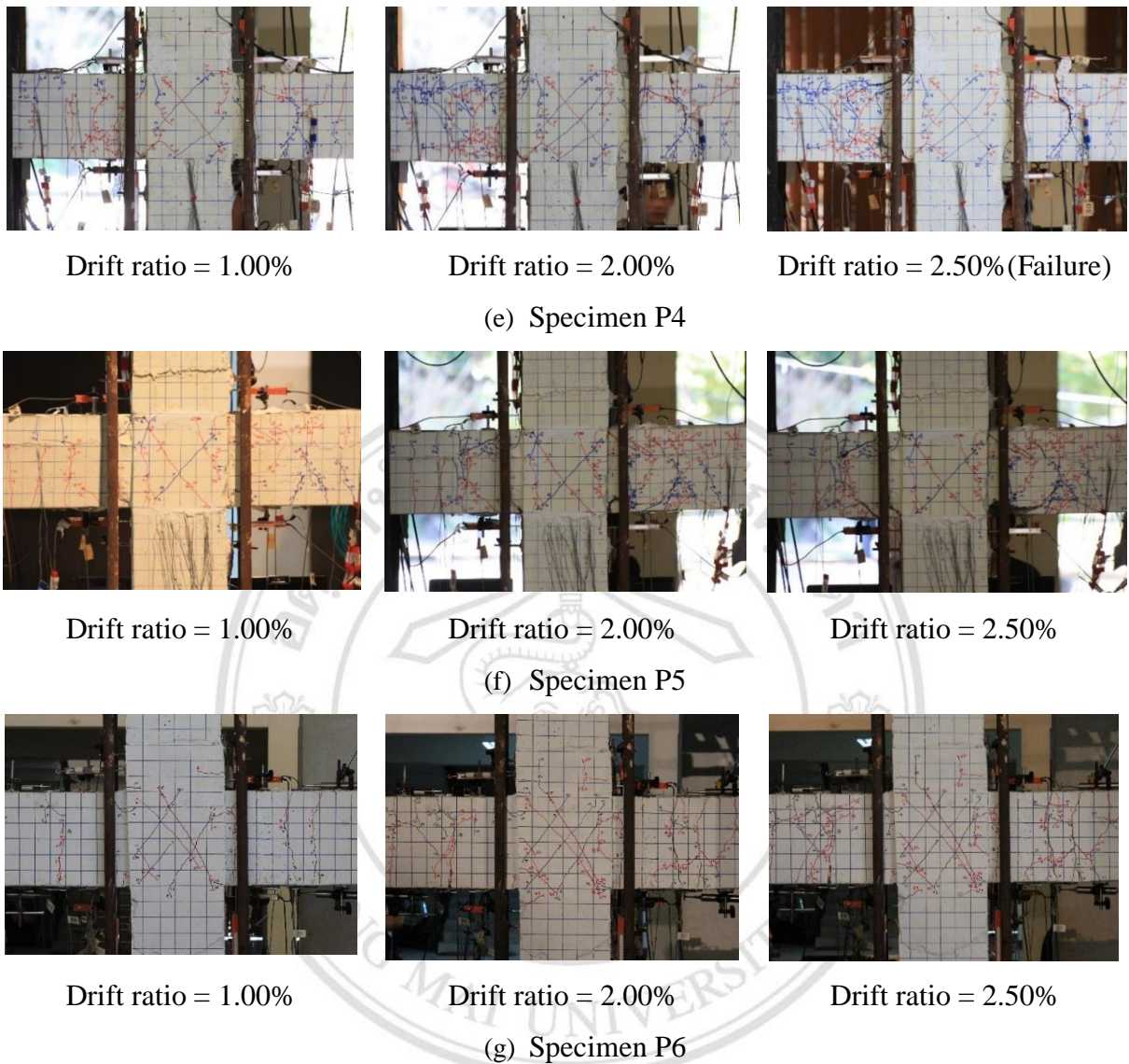


Figure 4.1 Crack patterns of all specimens

#### 4.1.1.1 Monolithic Specimen (M1)

The first flexural cracks on the bottom beams were observed at the column faces and a distance of 250 mm approximately away from the column faces, at the last cycle of 0.15% drift level. At 0.20 story drift, the flexural cracks on the top beam section appeared at the similar location of previous cracks on the bottom beam section. The first diagonal crack on the joint region and flexural cracks on columns were observed at the 0.50% story drift level. At the drift level reached to 1.40%, there were the flexural-diagonal combining cracks, appearing on the middle level of beam depth approximately located at 150 mm from beam-column interface. When the drift levels were continuously increased, those

cracks further propagated by concentrating on the joint core and the potential plastic hinge region on both beams. Spalling of cover concrete at the beam end appeared at the 3.50% story drift level. The bottom longitudinal beam reinforcements at the column face were bulged at the 4.00% story drift level. As shown in Figure 4.2, several diagonal and flexural cracks distributed over joint core and beam end region, respectively. The relationship of story shear and story drift response is presented in Figure 4.3. Hysteresis behavior of specimen M1 was good in term of ductility and energy dissipation. Pinching effect was not appear evidently on the reversed cyclic response. The ultimate lateral load capacities were 44.03 kN and 42.08 kN for push and pull directions, respectively.

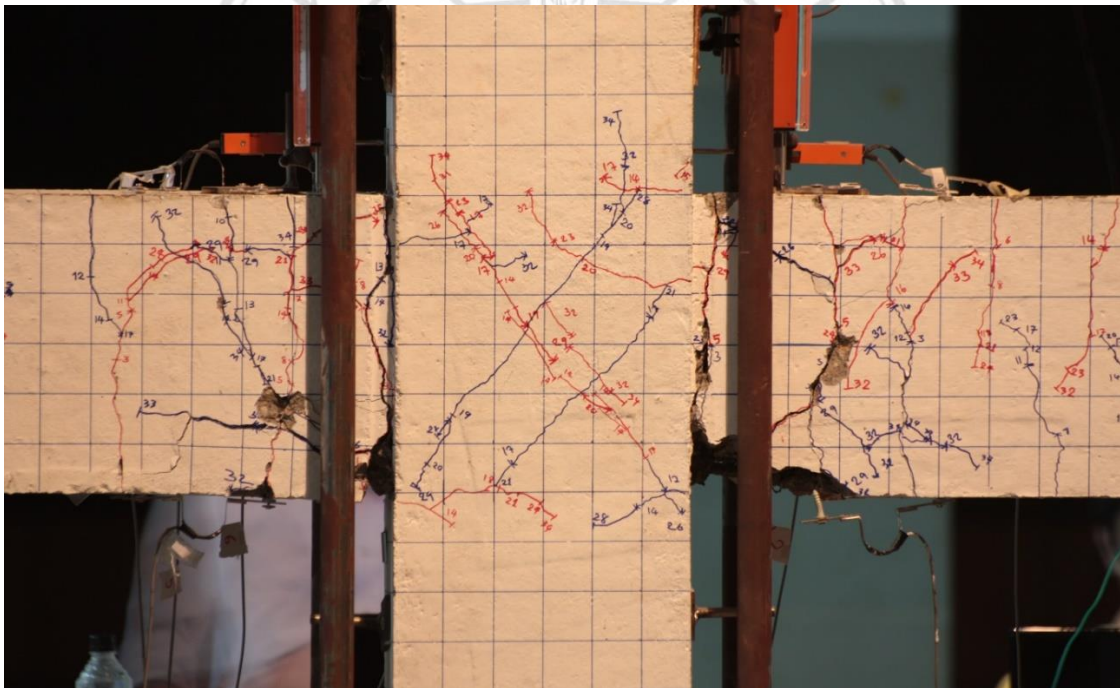


Figure 4.2 Damage level of specimen M1 at 4.00 percent story drift

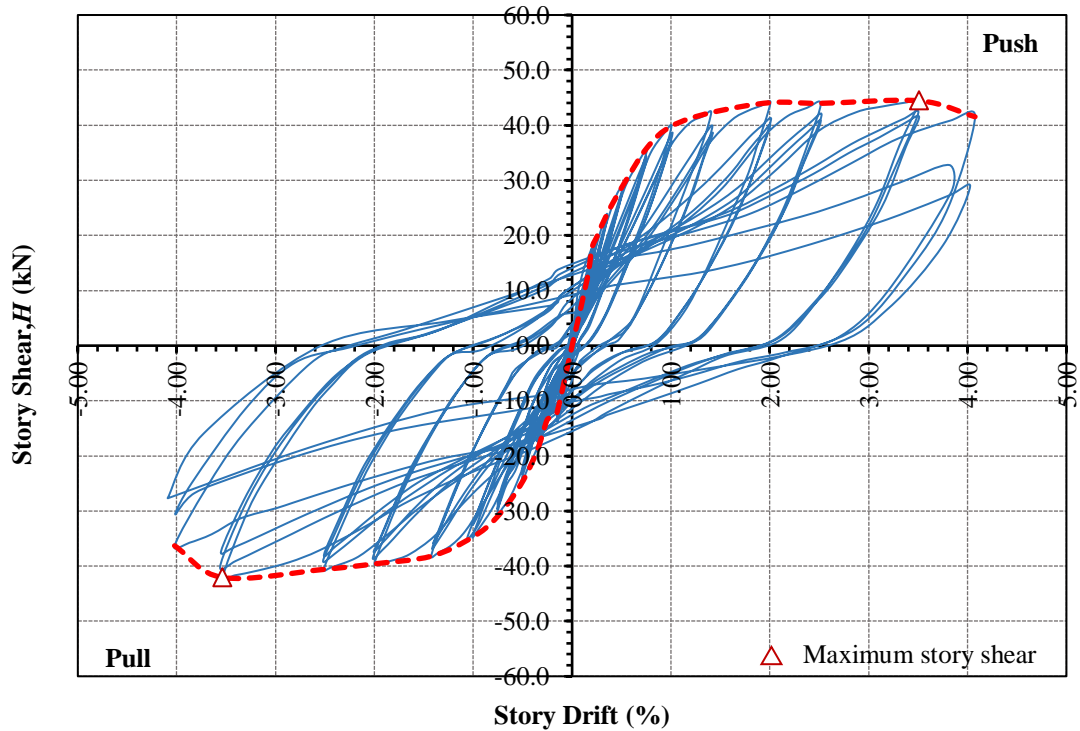


Figure 4.3 Story shear force vs. story drift ratio of specimen M1

#### 4.1.2 Current precast connection (Traditional connection detail, P1)

For the traditional precast concrete connection (P1) based on gravity design, a few vertical interface cracks from bottom beam along the beam depth of the beam-column interface, between precast beams and cast-in-place concrete joint, were observed at the 0.15% drift level. As the drift level rose to 0.25%, the first flexural crack appeared at the top beam section on high-strength grout concrete regions. At the drift levels of 0.35%, the first diagonal cracks were developed in the joint region and the horizontally splitting cracks parallel to the T-section steel inserted in the middle level of beam depth close to column face were started. The first flexural cracks on the bottom beams were generated at a distance of 300 mm approximately away from the column faces, at the first cycle of 0.50% drift level. During the drift level continuously reaching to 1.40%, those cracks progressively propagated, concentrating on the joint region and the potential plastic hinge beam regions. At the level of 1.40% story drift, the first splitting crack along the lap-splices on non-shrink grout concrete regions were formed within distances of  $d$  from the column face. After increasing the drift level up to 2.00-3.50%, those splitting cracks were gradually propagated and extended which they were wider than 2.0 mm. Furthermore, other flexural cracks on both beams were distinctly observed at the potential plastic hinge

regions near column face. Nevertheless, no crack appeared in the top and bottom column elements. Figure 4.4 shows the crack patterns of the specimen P1 after testing. The relationship of shear story and story drift level was shown in Figure 4.5. During reversal cyclic movements, hysteresis response exhibits severe pinching due to loss of bonding stress between longitudinal lap-splices and surrounding non-shrink grout. The maximum lateral capacities were 36.99 kN in push direction and 30.09 kN in pull direction. After the peak load, the story shear rapidly degraded due to the splitting cracks on the high-strength grout region and the middle level of the beam depth near the column face.

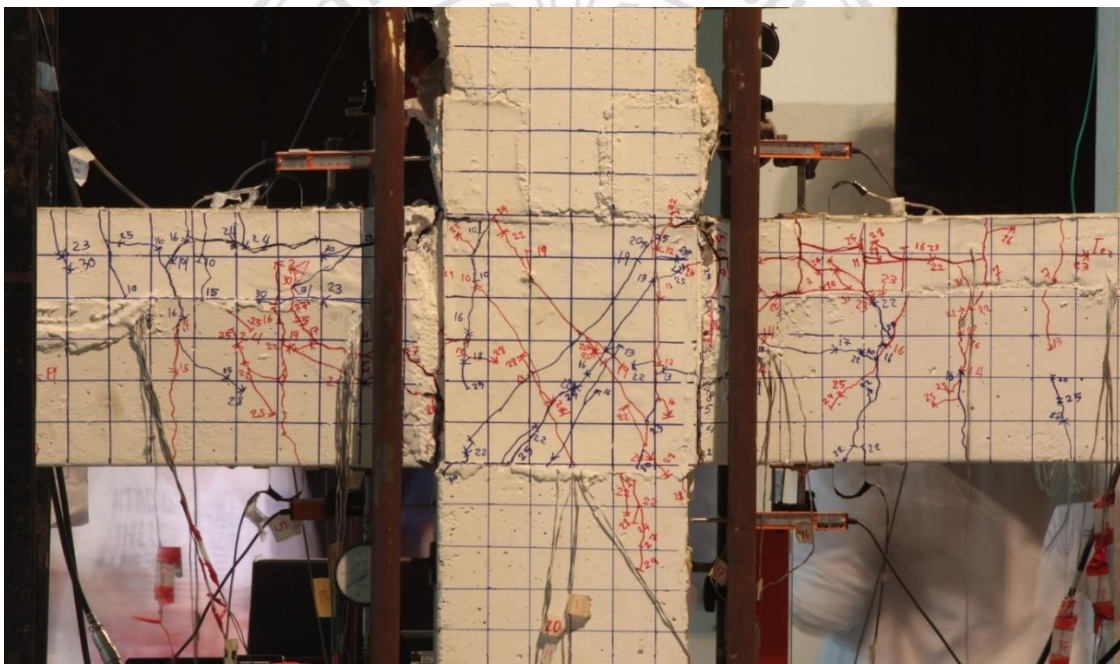


Figure 4.4 Damage level of specimen P1 at 3.50 percent story drift

Copyright © by Chiang Mai University  
All rights reserved

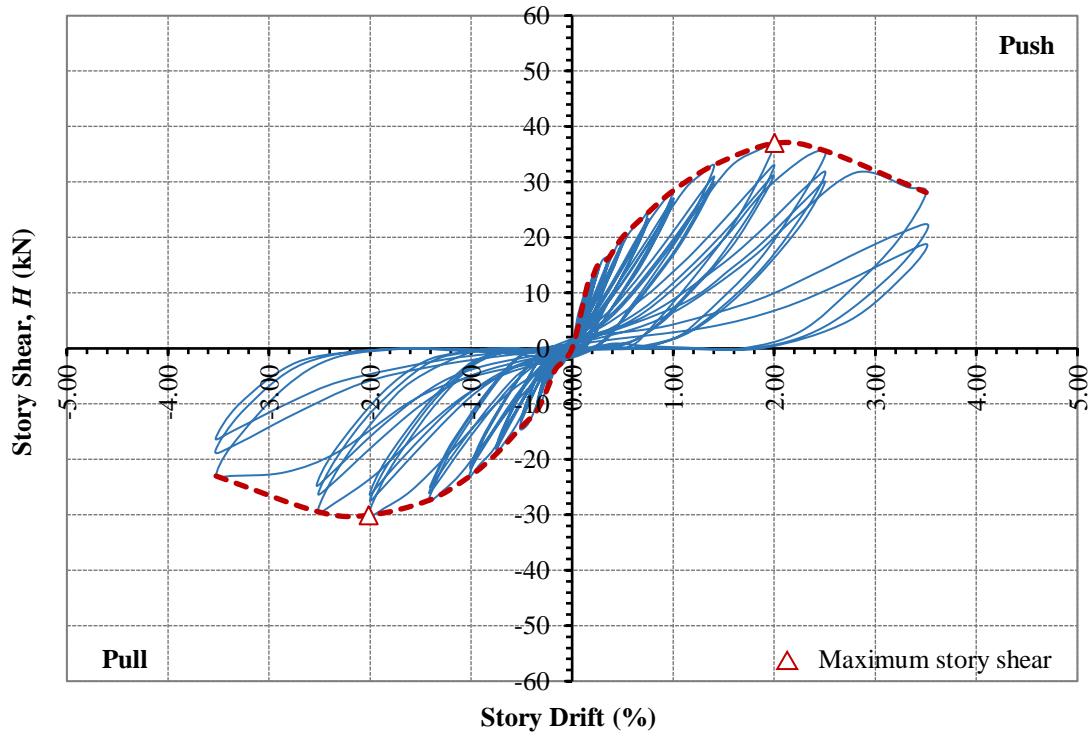


Figure 4.5 Story shear force vs. story drift ratio of specimen P1

#### 4.1.3 Modified precast connection (P2)

During testing specimen P2, first interface cracks appeared on the bottom beam at the column face during the second cycle in the 0.15% story drift level. There were flexural cracks on the beam at a distance of  $d/2$  from the column face, at the story drift level of 0.20%. Several flexural beam cracks were distributed over the plastic hinging zone during the 0.25%-0.35% drift levels. At the 0.50% drift level of both directions, the diagonal cracks were firstly established on beam-column joint region. With the drift level increased to 1.00%, visible lateral cracks were observed at the bottom beam elements at the beam end region in which the cracks penetrated into the joint region. Other flexural cracks on the beam were spread evenly. Furthermore, a few spitting cracks parallel to lap-splices at the top beam region were initiated at distances of 250 mm away from the precast concrete column corresponding to a drift level of 1.40%. Then, those spitting cracks were gradually propagated along the lateral directions, as the drift levels progressed. During story drift increment to 3.50%, the splitting cracks were gradually extended and wider than 2.0 mm, very similar to the P1 specimen. When the drift level



reached to 3.50%, the high-strength grout concrete at the top beam region close to the column faces started to crush and spall which formed along to the spitting crack. About cracking of the precast column, no crack appeared both top and bottom ones as shown in Figure 4.6. Figure 4.7 illustrated lateral story shear-displacement relation under cyclic loading. The ultimate loading capacities were 40.91 kN and 38.81 kN for push and pull cycles respectively. After the peak loads both push and pull directions, the lateral story shear dramatically dropped between 2.00% to 2.50% drift levels. After that, the backbone curve slightly decreased which the formation of the cure is similar to the bond failure curve, exhibiting the bond problem during quasi-static experiment.

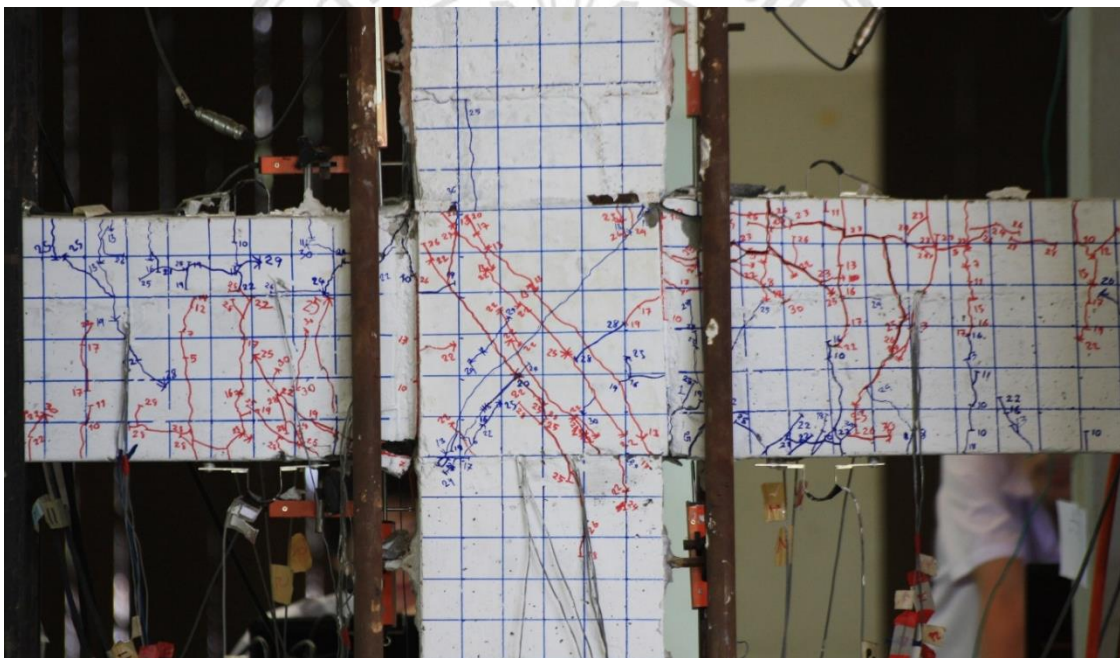


Figure 4.6 Damage level of specimen P2 at 3.50 percent story drift

Copyright © by Chiang Mai University  
All rights reserved

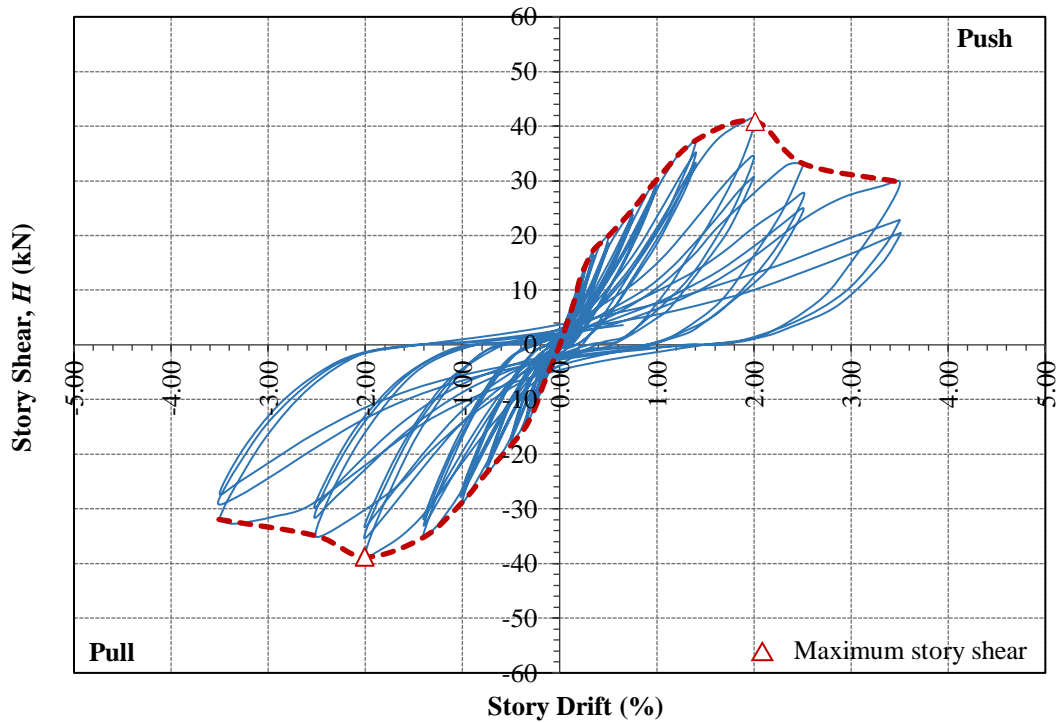


Figure 4.7 Story shear force vs. story drift ratio of specimen P2

#### 4.1.4 Modified precast connection (P3)

For the crack development during a quasi-static test of a precast specimen P3, a few flexural cracks in the plastic hinge beam regions were first observed during cyclic loading in the drift level of 0.20%. First diagonal cracks on the joint region appeared at the 0.25% drift ratio. The diagonal and flexural beam cracks were propagated at its locations during the drift levels up to 0.75%. While gradually rising to 1.40% of the levels of story drift, several diagonal cracks were obviously investigated, showing the development of truss or bonding mechanism in the joint core. At the 1.40% drift level, there were a few spalling of concrete cover on bottom beam region appearing at the beam-column interface. At the level of 2.00% story drift, there were also an appearance of horizontally splitting cracks parallel to lap splices on the non-shrink grout at top beam region as shown in Figure 4.8, representing the bond deterioration at the location. When the drift ratio reached to 2.50%, the splitting cracks were opened which was wider than 2.00 mm and a spalling of cover concrete in the grout concrete at the beam end region appeared as shown in Figure 4.9, causing serious damage to the bond stress in the high-strength grout concrete region. As a result of bonding damage in the critical

zone, the laterally strength capacities of a whole sub frame structure rapidly degraded after the peak load. A severe pinching effect shows in the hysteresis loop throughout the reversed cyclic response, exhibiting in Figure 4.10. The peak strength capacities were 38.52 kN and 32.63 kN for push and pull directions respectively.

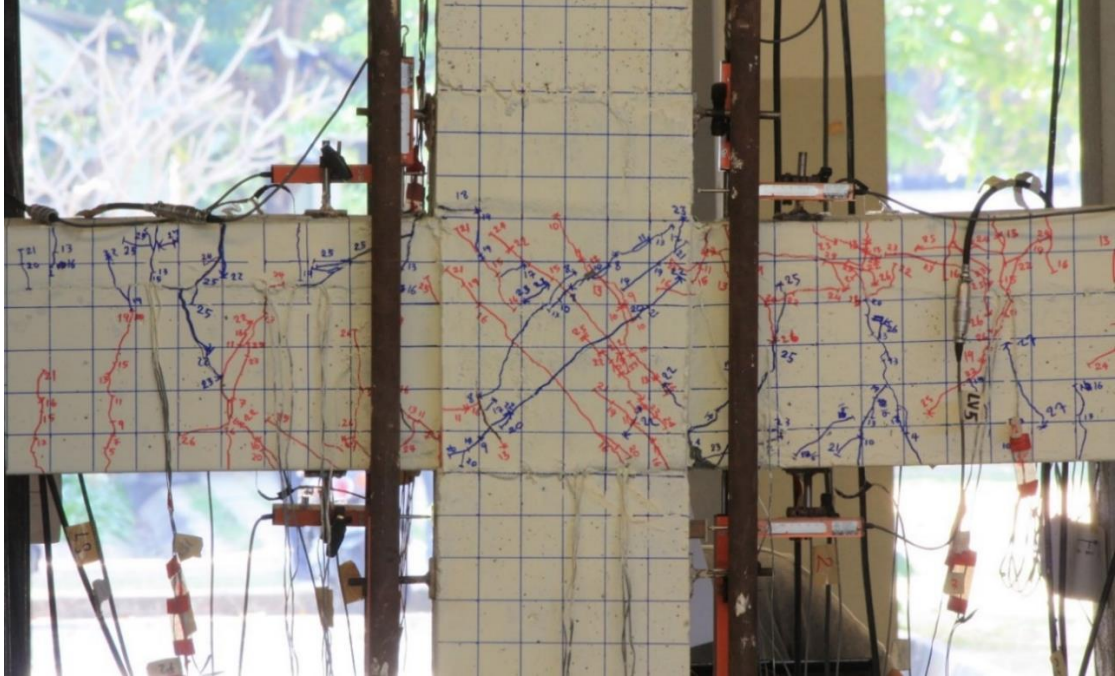


Figure 4.8 Crack distribution of specimen P3 at 2.00 percent story drift

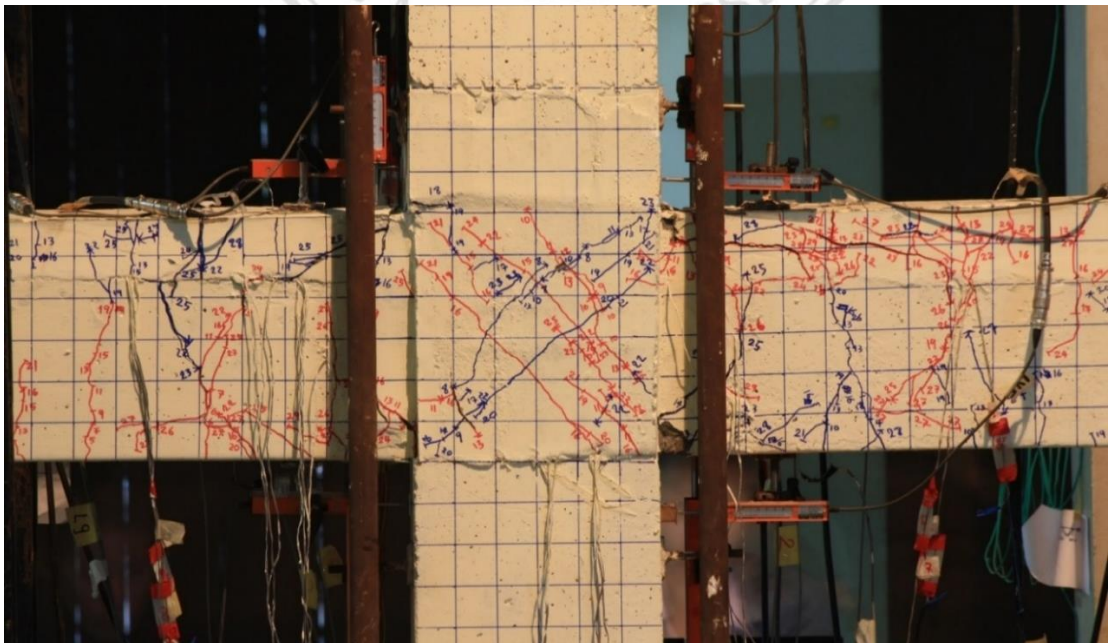


Figure 4.9 Damage level of specimen P3 at 2.50 percent story drift

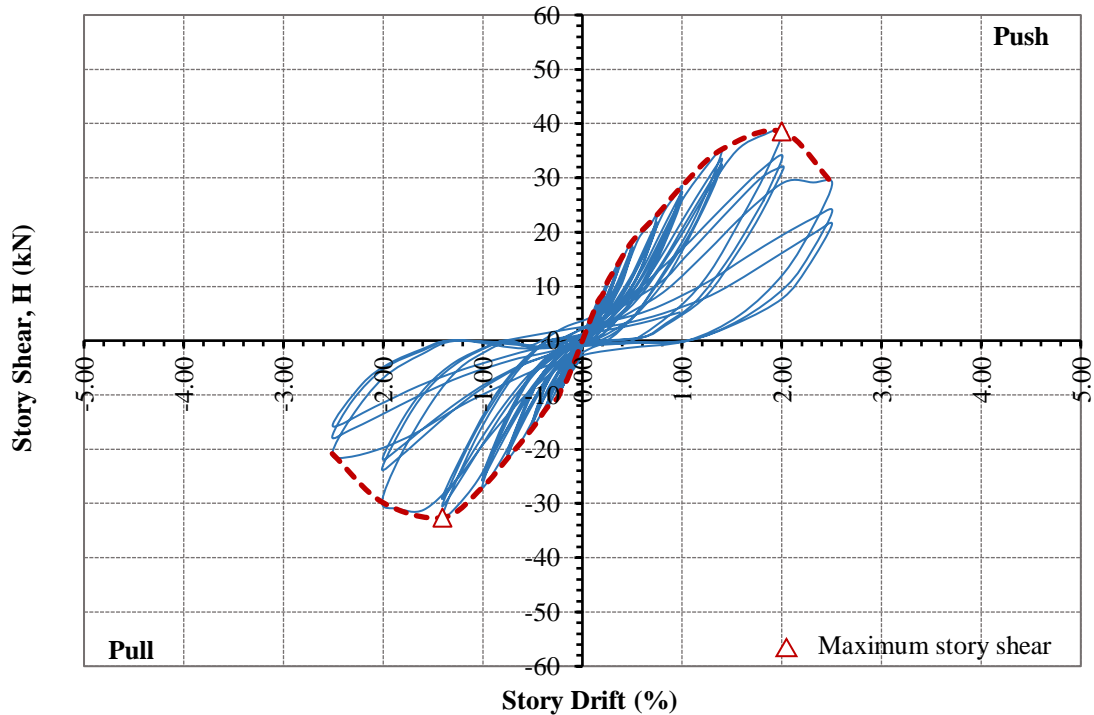


Figure 4.10 Story shear force vs. story drift ratio of specimen P3

#### 4.1.5 Modified precast connection (P4)

During the quasi-static testing of the precast specimen P4, first flexural cracks on both precast beams were observed at the  $d/2 - d$  distance from the column faces while the drift level grew up to 0.15%. A diagonal crack first appeared on the joint region at the 0.25% drift level. At the drift ratio of 0.75%, the horizontal cracks were investigated on the bottom beam region which these cracks penetrated into the joint region. The overall behavior of P4 specimen was very similar to that of P3 specimen up to the 1.00% story drift. During the drift levels reaching to 1.40%, splitting cracks on top and bottom beam regions were dramatically propagated. The additionally diagonal cracks were also observed over the joint region. At the 1.40% drift level, there were a few spalling of concrete cover on the bottom beam section at the column face. While the drift ratio played at the level of 2.00%, the splitting cracks along to lap splice on the high strength grout zone and the flexural cracks on the precast beam at the distance of  $d$  from the column faces were opened which were wider than 2.0 mm as shown in Figure 4.11. After that level, the lateral strength degradation in pull direction was more accelerated and pronounced, compared to the P3 precast specimen as shown in Figure 4.13. The

hysteresis response was very similar to the P3 precast specimen, showing the severe pinching effect throughout the reversed cyclic loading. The maximum loading capacities were 34.98 kN and 42.13kN for push and pull direction respectively. Figure 4.12 shows the crack distribution after the cyclic testing.

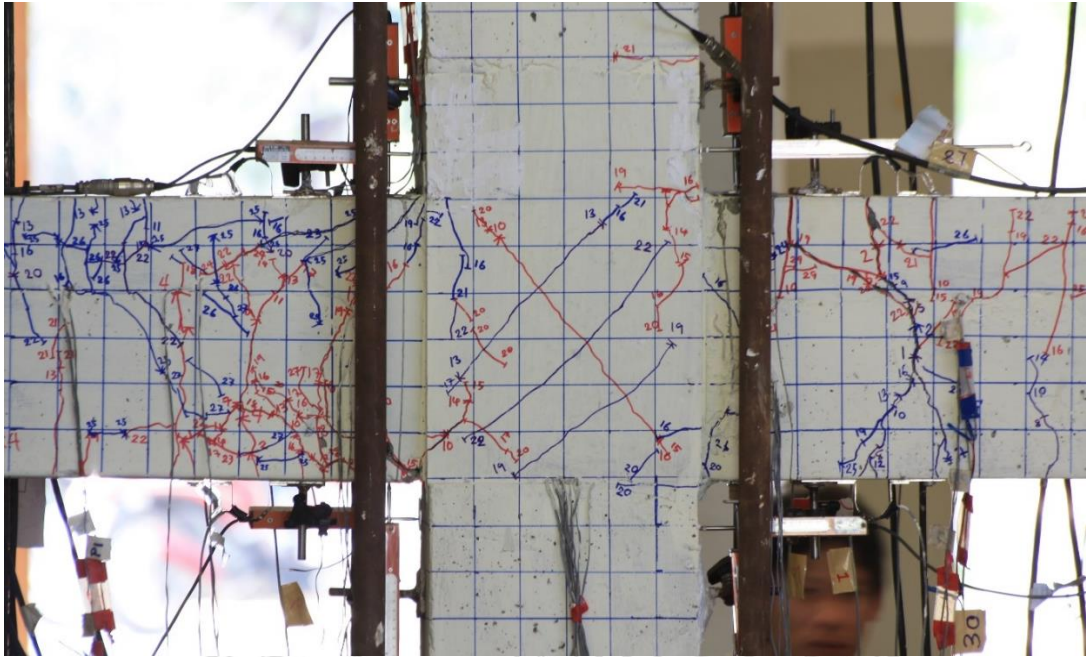


Figure 4.11 Crack distribution of specimen P4 at 2.00 percent story drift

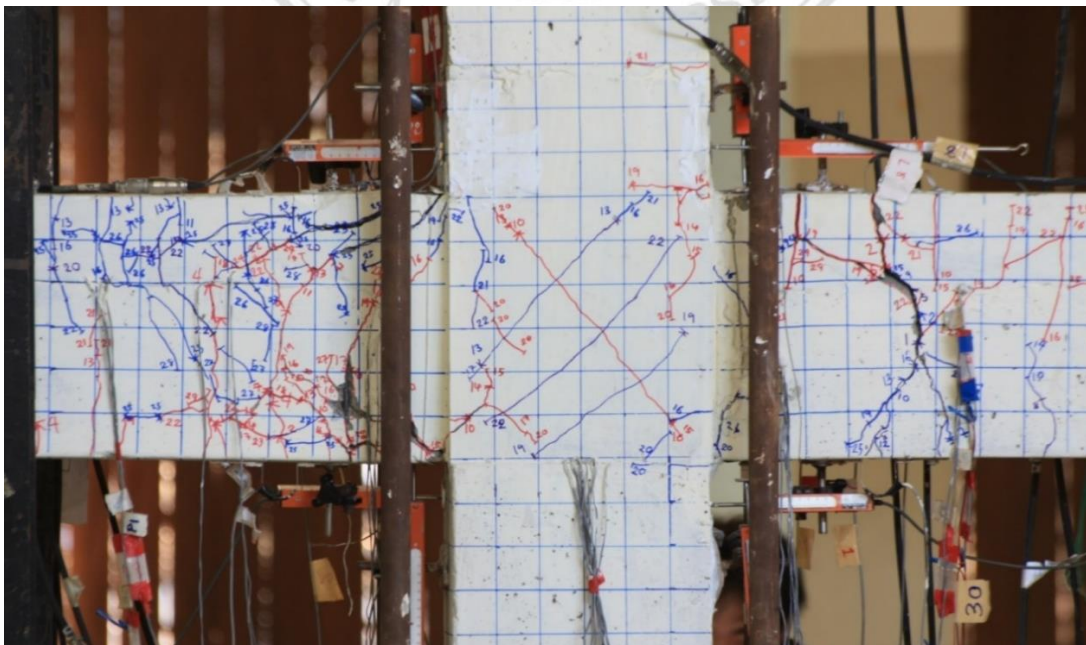


Figure 4.12 Damage level of specimen P4 at 2.50 percent story drift

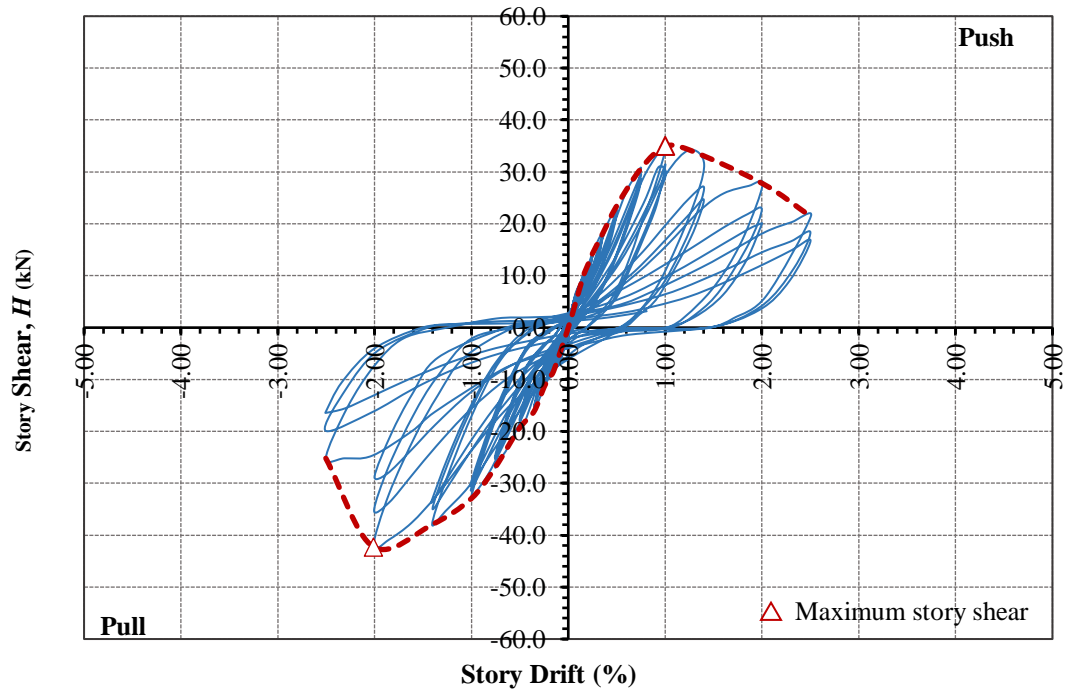


Figure 4.13 Story shear force vs. story drift ratio of specimen P4

#### 4.1.6 Modified precast connection (P5)

For the development of crack pattern during the cyclic quasi-static test of specimen P5, the first flexural crack was an interface crack observed along beam depth at the column face at the first cycle of the testing. At the 0.20% story drift level, the flexural cracks were developed on the beams at a distance of  $d$  from the column faces. Also, a few vertical cracks were first observed on joint core. There were a few diagonal cracks developed on the beam-column joint at 0.50 % drift level. During the story drift up to 1.40%, those flexural cracks over the beam, the vertical crack and diagonal cracks on the joint region gradually propagated. When the drift level was increased to 1.40%, the spitting cracks along to T-section steel and lap splice bars were initiated on the top and bottom beam region from the column face to the beam elements as shown in Figure 4.14. With the increase in the drift level runs, the spitting cracks further propagated until the concrete cover at below the T - section steel on the bottom beam region close to the beam-column joint were spalled which had direction coincidental with the spitting cracks corresponding to a drift level of 2.50%. At a distance of around  $d$  from the column face of the both precast beams, the concrete beams were separated from the flexural cracks with 1.0 mm width; moreover, spalling of concrete cover spread on the beam surfaces at

the location. Figure 4.15 shows the crack distribution of the specimen after testing. The plastic beam hinges were taken to distance of around  $d$  from the beam-column interface. Furthermore, the bond problem was observed by showing in the spitting crack pattern on the bottom beam region (below T-section steel connected to longitudinal beam bars) and a behavior of the backbone curve after the ultimate loads as shown in Figure 4.16. The recorded maximum capacities for push and pull directions were 40.92 kN and 36.82 kN respectively. The hysteresis loop showed a moderate pinching effect throughout the reversed cyclic response.



Figure 4.14 Crack distribution of specimen P5 at 1.75 percent story drift

Copyright © by Chiang Mai University  
All rights reserved



Figure 4.15 Damage level of specimen P5 at 3.50 percent story drift

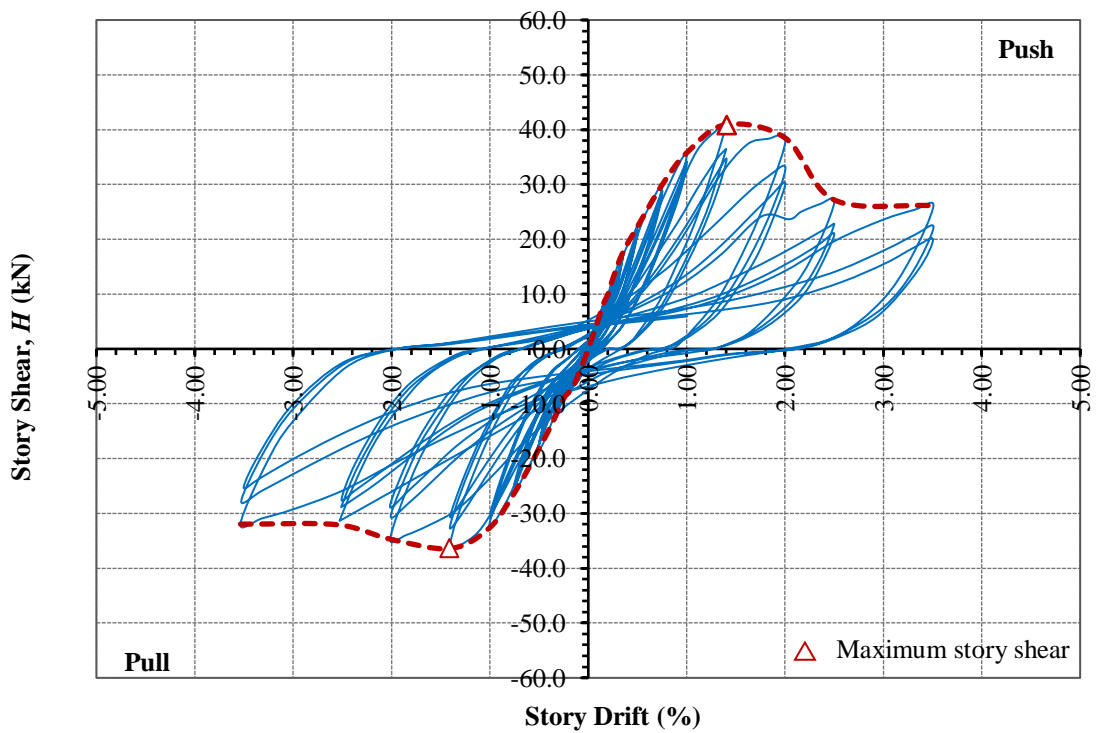


Figure 4.16 Story shear force vs. story drift ratio of specimen P5



#### 4.1.7 Modified precast connection (P6)

At the first drift level, the flexural cracks on both beams were observed in the location around the  $d-2d$  distance from the column faces. The first flexural crack at the beam-column interface was developed, when the story drift was at 0.20%. At the drift level of 0.35%, a diagonal crack in the joint region obviously appeared. During 0.50%-1.00%, several flexural cracks were well distributed over the beam region at the distance of  $d-2d$  from the beam-column adjacent. There were another diagonal cracks appearing in the joint core, representing a combination of diagonal strut and truss mechanisms. First diagonal cracks on both precast beams located about 30 cm away from the column face were observed at the 1.40% story drift. At the 2.00% drift level, there were horizontal cracks in level of cover concrete on top beam region, located around the distant  $d$  away from the precast column. A few spalling concrete cover in bottom precast beam region were investigated located around 20-25 cm away from the column face at the story drift level of 2.50%, coinciding the edge of T-section steel insert in precast beams. When the drift level reached 3.50%, the flexural cracks of beam elements located around 20-25 cm away from the column face were opened approximately 2.0 mm width, widening of the cracks accelerated at repeated cycle in the same drift level. Also, the horizontal cracks wider than 2.0 mm further propagated, running from the column face along 25 cm to the flexural beam cracks as shown in Figure 4.17. At the first cycle of the 4.50% story drift level, concrete beam structures at the edges of T-section were separated due to the flexural crack opening. Afterward, the spalling of concrete cover on the top and bottom beam regions at the location was observed. With the quasi-static test in the last cycle as shown in Figure 4.18, other spalling of concrete cover spread on the beam surfaces at the edges of T-section region. The critical beam region was successfully moved approximate one effective beam depth away from the column faces. Regard to the crack pattern in the precast column elements, there were a few flexural cracks appearing at the interfaces of beam and column. Figure 4.19 shows the hysteresis behavior and envelope curve of the P6 precast specimen. The hysteresis response was very similar to monolithic specimen M1. There was no observation of pinching effect throughout the reversed cyclic response. The ultimate lateral load capacities for push and pull directions were 50.07 kN and 46.60 kN respectively.

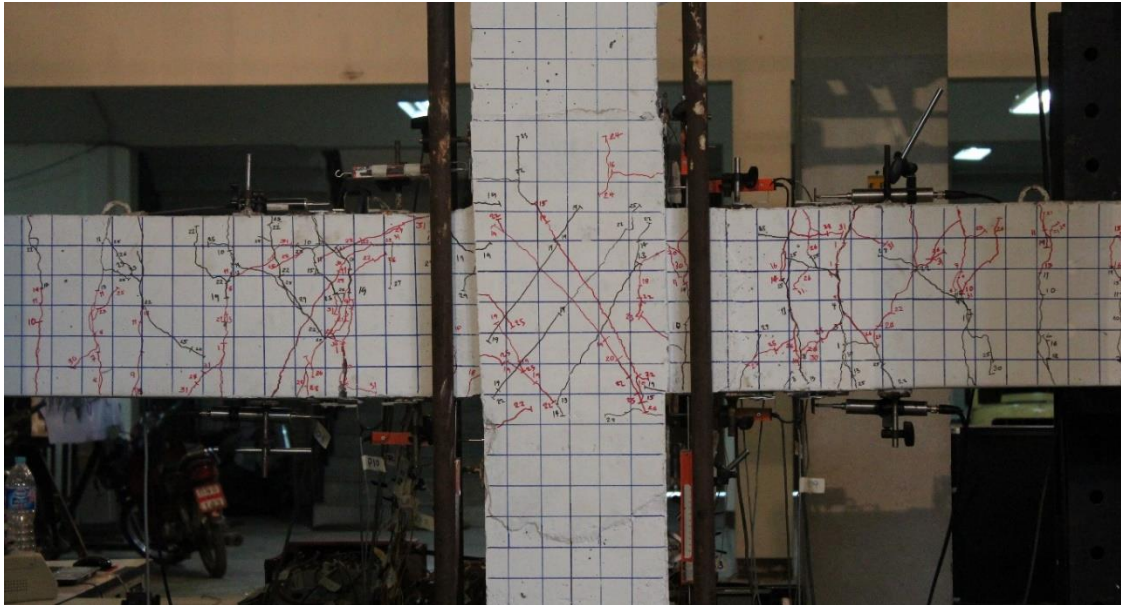


Figure 4.17 Crack distribution of specimen P6 at 3.50 percent story drift

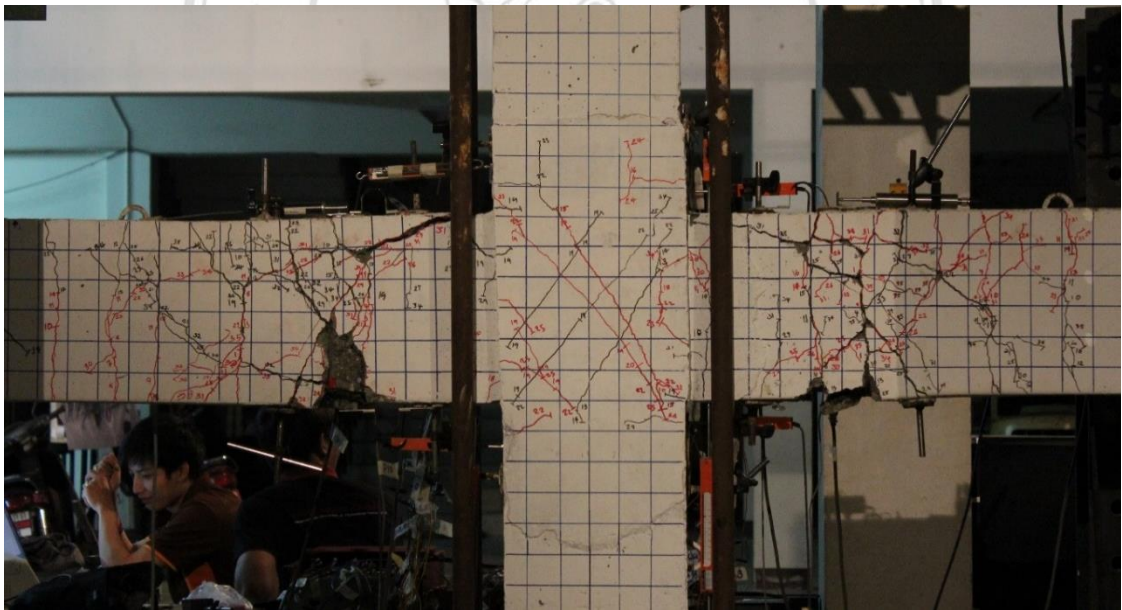


Figure 4.18 Damage level of specimen P6 at 4.50 percent story drift

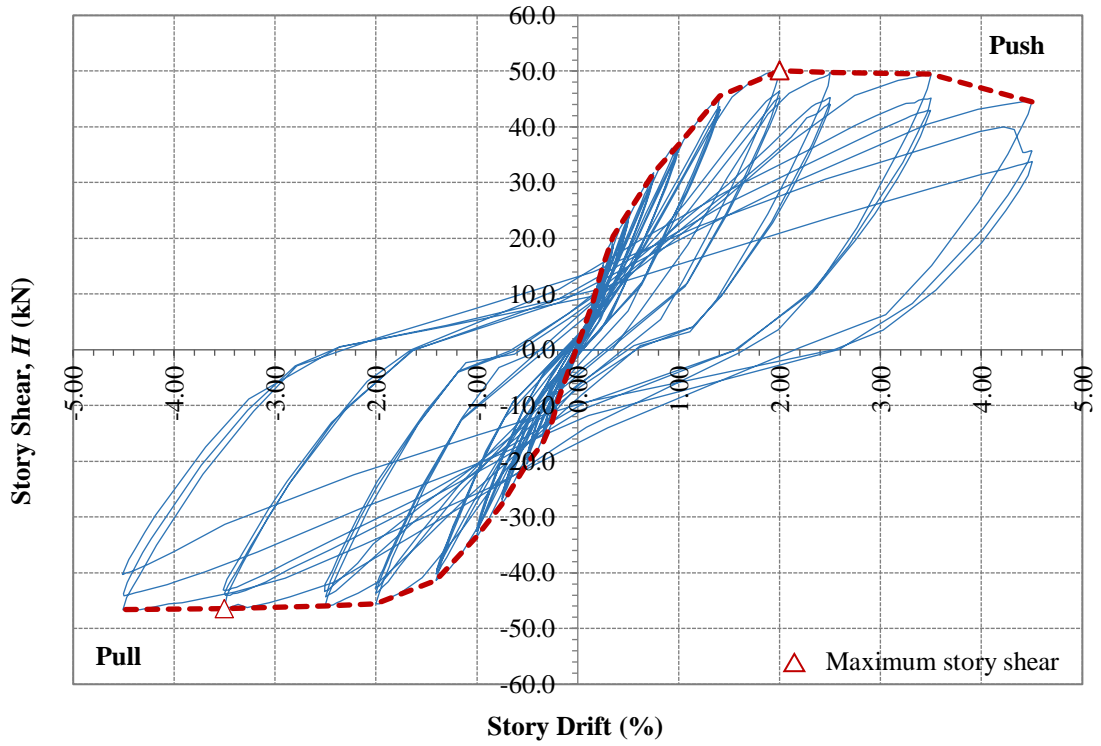


Figure 4.19 Story shear force vs. story drift ratio of specimen P6

ลิขสิทธิ์มหาวิทยาลัยเชียงใหม่  
 Copyright© by Chiang Mai University  
 All rights reserved